IEEE Access
Multidisciplinary | Rapid Review | Open Access Journal

Received August 15, 2020, accepted September 7, 2020, date of publication December 31, 2020, date of current version January 5, 2021.

Digital Object Identifier 10.1109/ACCESS.2020.3026552

Online State-of-Health Estimation for Second-Use Lithium-Ion Batteries Based on Weighted Least Squares Support Vector Machine

WEI XIONG[1,2], YIMIN MO[2], AND CONG YAN[2]
[1]School of Mechanical Engineering, Hubei Engineering University, Xiaogan 432000, China
[2]School of Mechanical and Electronic Engineering, Wuhan University of Technology, Wuhan 430070, China

Corresponding author: Yimin Mo (174181461@qq.com)

This work was supported by Manufacturing Industry Development Research Center on Wuhan City Circle, Jianghan University, under Grant WZ2020Y04.

ABSTRACT Online state-of-health (SOH) estimation is critical for second-use retired lithium-ion batteries. However, the SOH of retired batteries is highly nonlinear, and the existing degradation trend data are limited. Consequently, achieving accurate and effective SOH estimation remains a challenge. To address the above problem, an online SOH estimation based on a weighted least squares support vector machine (WLS-SVM) is proposed in this paper. In this work, the health features (HFs) are first extracted from the partial charging curves of retired batteries, and the Pearson correlation coefficient is applied to select the important HFs that are strongly correlated to the SOH. These selected HFs are used as the estimation model inputs for characterizing the aging procedure of the retired battery effectively. Then, to enhance the accuracy and robustness of SOH estimation, the standard support vector machine (SVM) is improved by a weighting function and linear equations. Last, the online SOH estimation is conducted by using the test data sets of second-use batteries with different battery materials and under different conditions. The results show that compared with the most popular methods, such as the back-propagation neural network (BPNN)-based method, the Gaussian process regression (GPR)-based method, and the standard SVM-based method, the performance of the WLS-SVM-based method is superior. The root mean square error (RMSE) for the SOH estimation with the WLS-SVM-based method for all the test cells is less than 1.85% at different aging paths and levels, whereas the RMSEs of the BPNN-based method, GPR-based method, and standard SVM-based method are within 3.6%, 5.7%, and 7.6%, respectively. The proposed WLS-SVM-based method can thus provide highly robust and accurate online SOH estimation.

INDEX TERMS Electric vehicles, second-use lithium-ion battery, online SOH estimation, WLS-SVM, HF.

NOMENCLATURE

A. ABBREVIATIONS

SOH	state-of-health
WLS-SVM	weighted least squares support vector machine
HF	health feature
SVM	support vector machine
BPNN	back propagation neural network
GPR	Gaussian process regression
EV	electric vehicle
EKF	extended Kalman filter
RBF	radial basis function
NMC	$Li(NiCoMn)O_2$
IC	incremental capacity
CC	constant current
MSE	minimal square error
MAE	mean absolute error
RMSE	root mean square error

B. SYMBOLS

$\rho_{SOH,HF}$	Pearson correlation coefficient between SOH and HF
C_t	the capacity of the t-th cycle

The associate editor coordinating the review of this manuscript and approving it for publication was Moussa Boukhnifer.

C_N	the nominal capacity
C	the penalty parameter
ξ_i	slack variable
a_i	Lagrange multiplier
$K(x_i, x)$	the kernel function
γ	the radius of the radial basis kernel function
$f(x_i)$	the estimated SOH
y_i	the actual value
l	the number of samples
v_i	the weight vector of WLS-SVM
$\hat{S}$	the standard deviation,
$MAD(e_i)$	the median absolute deviation
I	the identity matrix

I. INTRODUCTION

As more electric vehicles (EVs) have appeared on roads, the disposal of EV batteries has become an increasing concern [1]. When the energy storage capacity of an EV battery declines to 80%, the battery is no longer suitable for EVs and must be replaced [2]. It is estimated that the number of retired EV batteries will reach approximately 10,446 tons in China alone by 2020 [2], [3]. If the used EV batteries cannot be handled appropriately, it will not only waste resources but also cause great harm to the environment. It is essential to deal with retired batteries reasonably. Although retired battery packs do not meet the requirements for EVs, most the battery cells are still healthy and fully functional [4]. Accordingly, instead of disposal, reusing is regarded as the best way to deal with the retired batteries [5]. Currently, retired batteries are usually repurposed in residential energy storage devices, which have a lower peak power demand and relatively smooth energy consumption. To safely and efficiently use retired batteries, an accurate state estimation is critical to assess their second-life service. An online state-of-health (SOH) estimation is the most important deciding factor for ensuring the safety of the second-use retired batteries.

The SOH is a battery age metric that reflects the ability of a battery to store and deliver energy relative to its initial condition [6]. It can be expressed as:

$$SOH = \frac{C_t}{C_N} \tag{1}$$

where C_t is the capacity of the t-th cycle and C_N is the nominal capacity. The battery aging rate depends on the battery operation state, including charging and discharging rates, the depth of discharge, and the external environment, such as ambient temperature and storage conditions [7]. A clear understanding of second-use battery aging information can help users improve second-use battery application conditions and avoid the occurrence of safety hazards. Therefore, researchers have made great efforts to develop SOH estimation methods.

In recent years, studies on SOH estimation have increased [7], [8] and have been classified into model-based methods and data-driven methods [9]. Model-based methods, including equivalent circuit models and electrochemical models, consider the degradation process, and the failure mode is applied to estimate battery SOH. Wang *et al.* [10] estimated the battery SOH by using a state-space model of the discharge rate. Relying on an empirical model [11], Yu *et al.* [12] applied a particle filter to estimate battery SOH. Kim and Cho [9] employed a battery equivalent circuit model and used the extended Kalman filter (EKF) method to estimate the SOH. Guha [13] proposed a fusion method for SOH prediction that combines a capacity reduction model and an internal resistance growth model. However, these model-based methods require complex computations and a large amount of prior knowledge to describe the degradation mechanism and material properties, so it is difficult to achieve online estimation. The data-driven approach is an efficient and effective method. Data-driven methods extract the hidden information and evolution rules from the battery data to realize the online SOH prediction of lithium-ion batteries, which do not require accurate physical models [14], [15]. Liu *et al.* [16] predicted the battery SOH by using a Gaussian process regression (GPR)-based method. Li *et al.* [17] presented an SOH estimation approach by combining an ensemble learning neural network with a characteristics analysis of the charge-discharge curve [18]. Yang *et al.* [19] selected a three-layer back-propagation neural network (BPNN) to obtain an accurate SOH estimation. He *et al.* [20] estimated the battery SOH online by using dynamic Bayesian networks to give reasonable prediction results. Although these present data-driven methods can improve the estimation accuracy to some extent, they require sufficient training data, which is difficult to achieve in practical applications [21], [22]. Additionally, the SOH of a second-use battery is strongly nonlinear. These methods have difficulty obtaining good estimation results with limited samples.

To overcome the above problems, the support vector machine (SVM) has been proposed because it is more suitable for nonlinear problems with a small number of samples. Chen *et al.* [7] proposed an SVM with a radial basis function (RBF) as the kernel function to estimate the SOH. Xu *et al.* [23] identified the battery SOH using an SVM. In the above studies, the SVM can provide good estimation results under specific working conditions, but the robustness of the SVM is poor because it can be easily misled by abnormal training points. An SVM only selects a few data points as support vectors for training. If there are abnormal training points in these data, the estimation error based on the SVM method will increase significantly.

To improve the estimation performance, a weighted least squares support vector machine (WLS-SVM)-based method is proposed in this paper. The purpose is to achieve a trusted online SOH estimation for second-use lithium-ion batteries with limited training data sets. The WLS-SVM-based method takes all training data as support vectors to fully characterize the deterioration of second-use lithium-ion batteries and uses a weight function to weight error variables, which can obtain SOH estimation with high accuracy. The robustness and feasibility of the proposed WLS-SVM-based method

TABLE 1. The tested cells.

Battery number	Cell chemistry	Nominal capacity	Remaining capacity
B1	NMC	2.4Ah	1.94
B2	NMC	2.4Ah	1.93
B3	NMC	2.4Ah	1.93
B4	NMC	2.4Ah	1.94
B5	NMC	2.6Ah	2.10
B6	NMC	2.6Ah	2.09
B7	$LiFePO_4$	2.6Ah	2.09
B8	$LiFePO_4$	2.6Ah	2.09

are systematically validated by applying test data sets from different battery materials under different conditions.

The main contributions of this study are twofold: (1) First is the construction and selection of health features (HFs). Considering the effective extraction of HFs in practical applications, we select the charging capacity as the HF from partial charge profiles. The HFs we select are not affected by the change in charging current rate. The Pearson correlation coefficient is applied to determine the key HFs that are strongly correlated to the SOH. Then, using the key HFs as the estimation model input, the aging of the retired battery can be reflected effectively. (2) Second is the development and verification of the WLS-SVM model. We improve the standard SVM with a weighting function and linear equations, allowing the estimation model to fully characterize the deterioration of second-use lithium-ion batteries and reduce computational complexity. Then, applying several second-use lithium-ion battery data sets with different conditions and different battery materials, the SOH estimation is conducted and compared with the most popular SOH estimation methods to verify the proposed method.

The remainder of this paper is organized as follows. Section 2 describes the methodology, which includes healthy feature selection and the WLS-SVM-based method. The SOH estimation results and a discussion are offered in Section 3. Section 4 presents the conclusions.

II. METHODOLOGY

A. THE METHOD FRAMEWORK

To enhance the performance of online SOH estimation, this paper proposes a WLS-SVM-based method. As shown in Fig. 1, the proposed method can be implemented in three steps: feature selection, offline modeling, and online estimation. First, HFs are selected based on Pearson correlation coefficients. Second, the WLS-SVM model is trained offline by using data sets that involve HFs and real SOH. Finally, taking the test data sets as input, the WLS-SVM model is used to estimate the SOH online.

B. HEALTHY FEATURE SELECTION

Because it is difficult to build a direct mapping relationship between the second-use battery SOH and the measured data, it is crucial to select appropriate healthy features for the SOH in the characterized second-use battery. In this section, by introducing second-use battery experiments, the key HFs are determined by the Pearson correlation coefficient, which can evaluate the correlation between the HFs and the target.

TABLE 2. Experimental conditions of the batteries.

Battery number	Charging/discharging current rate	Voltage upper	Voltage lower	Cut-off current
B1, B2	0.5C/0.5C	4.2 V	2.7 V	0.05C
B3, B4 B5, B6	0.5C/1C	4.2 V	2.7 V	0.05C
B7, B8	1C/1C	3.65V	2.5 V	0.05C

1) LITHIUM-ION BATTERY DATA

In this work, $Li(NiCoMn)O_2$ (NMC) and $LiFePO_4$ batteries are obtained from the retired battery packs of several pure electric passenger cars. These EVs had been used for over three years, and their mileage was over 35,000 km. The retired batteries still possessed approximately 80%-85% of their initial capacities. Before the life cycle tests, we screened the batteries for consistent capacity. Table 1 presents the remaining capacities and the nominal capacities of these batteries.

We divided these batteries into three groups to conduct life cycle tests under different load profiles. A schematic of the test bench is shown in Fig. 2. It consists of a Bitrode MCV12-100 for the battery test, a thermal chamber for environmental control and a host computer for operational control and data display/storage. The experiments were carried out at room temperature, and the experimental conditions of the second-use batteries are shown in Table 2. The retired batteries are mostly used under a low current rate during second use [1], so the maximum discharge current rate we selected is 1C. The charging current rates we chose include 0.5C and 1C.

To obtain the degradation trends of second-use battery SOHs under different conditions, we select the data sets of B1, B3, B5, and B7, which are used to train the WLS-SVM model. We select the data sets B2, B4, B6, and B8 to test the performance of the proposed method.

2) FEATURE EXTRACTION

The HF is crucial in determining the performance of the SOH estimation method; therefore, the HFs are analyzed and extracted in this section. Generally, battery degeneration is primarily influenced by its working voltage, current and temperature, and its degeneration degree is also represented by changes in these three characteristics [24]. Thus, the main problem is when and how to acquire these measurements.

When comparing the charge and the discharge conditions, the discharging process is volatile, which makes it difficult to extract HFs. As a result, hidden information during charging is often seen as an important healthy feature because the charging process is relatively stable. Li *et al.* [25] selected incremental capacity (IC) curves during charging as the

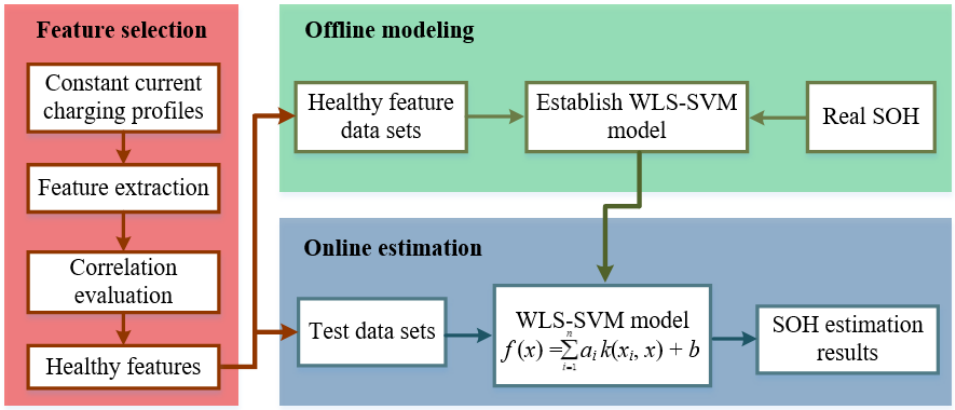

FIGURE 1. Overall view of the proposed SOH estimation method.

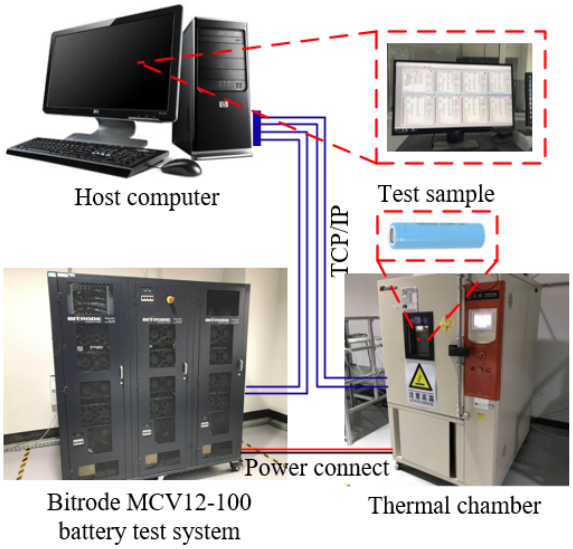

FIGURE 2. Schematic of the test bench.

healthy indicator. It can be seen that the IC peaks at different aging states have unique shapes, amplitudes and positions, which is a key for indicating the SOH through the change of the peaks [26]. However, the limitations of the incremental capacity analysis, such as requiring a low current rate for measurement, eliminating the noise of the curves, and engaging a high computational effort for the microcontrollers, are hard to overcome in practical applications. Li *et al.* [17] selected the ratio of constant current (CC) during the charging phase and the time spent in the selected equidistant voltage interval as the healthy features. Chen *et al.* [27] chose the CC mode duration as the input feature in their proposed method. Zheng and Deng [28] took the area under the CC mode, the time duration from 3.9 V to 4.2 V under the CC mode and the end time of the CC mode as the training data sets. The CC charging process is more stable, and the representative features can be extracted to create a more accurate SOH estimation model. Nevertheless, there is little chance for full charge or discharge during practical applications [23]. Therefore, it is difficult to obtain the ratio of the CC mode, the CC mode duration, and the end time of the CC mode for online SOH estimation.

Utilizing the partial charge curves to estimate the online SOH of second-use batteries is more practical [29]. Feng *et al.* [23] estimated the SOH by comparing the similarities of the charging voltage segment curves, which essentially compares the geometrical characterizations. Whereas this approach showed very good performance under constant charging current conditions, it is difficult to guarantee the correlation between SOH and geometrical characterization when the current rate changes, such as when the charger is replaced. Meng *et al.* [30] selected several voltage ranges as healthy features to estimate the SOH. This approach provides more flexibility for SOH estimation, but the correlation between battery SOH and each selected voltage range is not always the strongest. Therefore, in practical applications, the healthy features extracted from partial charge profiles with high correlations to the battery SOH are the best inputs to the training model for SOH estimation accuracy [31].

To select the healthy features from partial charge profiles, we examine the charging curves. Fig. 3 shows the charging voltage and current curves of battery B1 at SOH 80%, SOH 75%, SOH 70%, SOH 65%, SOH 60%, SOH 55%, and SOH 50%. Although the current in the CC charging stage is the same as shown in Fig. 3(b), the slopes of the second-use battery voltage curves are different under different battery degeneration degrees, as shown in Fig. 3(a).

In a certain voltage range, the different slopes of the voltage curves result in different charging times and charging capacities, as shown in Fig. 4. Nevertheless, under the same temperature, the charging time will be changed when the charger is replaced or the battery degenerates. The charging capacity is only affected by battery degeneration. A further analysis of the charging curves for different degeneration degrees reveals that in the CC phase, the different battery degeneration degrees will lead to inconsistent charging capacities at different voltage intervals. Therefore, we can speculate that there is a certain correlation between the SOH and the

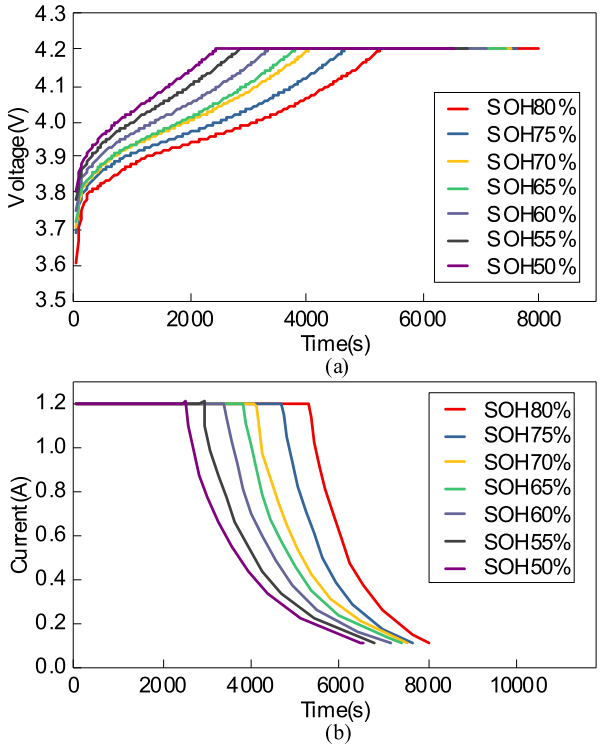

FIGURE 3. Charge profiles of B1 with different SOHs. (a) Charging voltage. (b) Charging current.

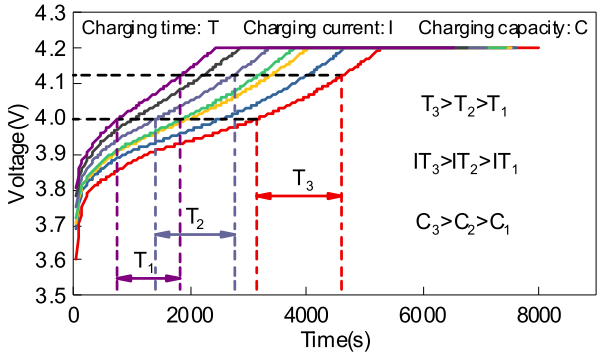

FIGURE 4. Charging curves.

charging capacity at different voltage intervals. Based on this conclusion, 8 HFs can be extracted from the CC charging phase:

HF1: the charging capacity from 3.8 V to 3.85 V under the CC mode.

HF2: the charging capacity from 3.85 V to 3.9 V under the CC mode.

HF3: the charging capacity from 3.9 V to 3.95 V under the CC mode.

HF4: the charging capacity from 3.95 V to 4 V under the CC mode.

HF5: the charging capacity from 4 V to 4.05 V under the CC mode.

HF6: the charging capacity from 4.05 V to 4.1 V under the CC mode.

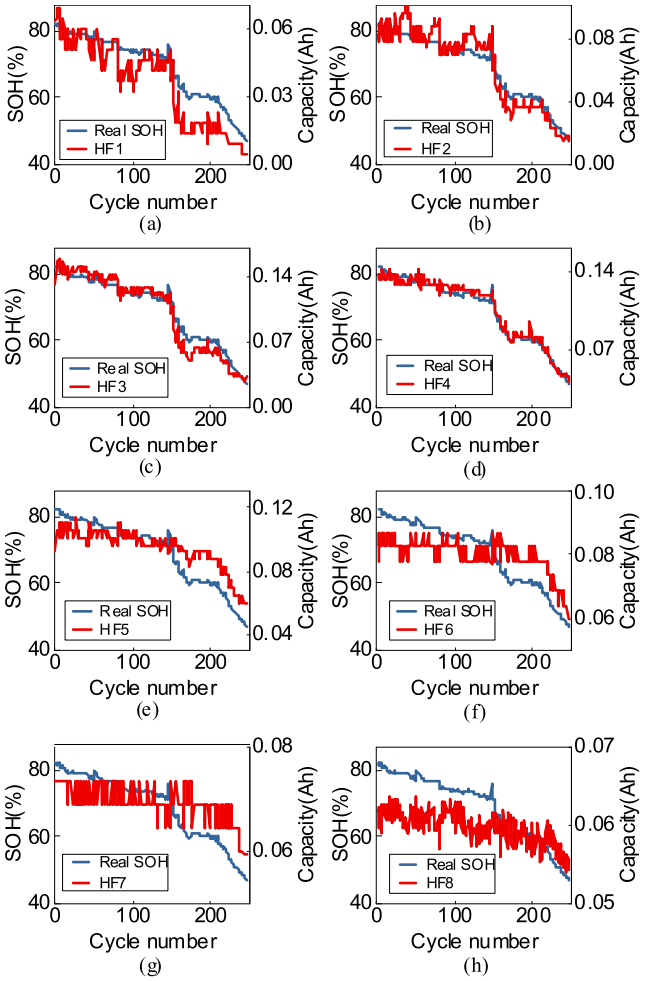

FIGURE 5. Effects of second-use battery degeneration on HFs. (a) HF1. (b) HF2. (c) HF3. (d) HF4. (e) HF5. (f) HF6. (g) HF7. (h) HF8.

HF7: the charging capacity from 4.1 V to 4.15 V under the CC mode.

HF8: the charging capacity from 4.15 V to 4.2 V under the CC mode.

Due to the characteristics of the second-use battery charging voltage at SOH 50%, the voltage intervals are divided from 3.8 V. The CC charging phase from 3.8 V to 4.2 V is divided into 8 voltage intervals, with 0.05 V for each interval The charging capacities during these 8 voltage intervals are regarded as health features and named HF1-8.

The effects of second-use battery degeneration on HFs are shown in Fig. 5. The HFs of the second-use battery decrease with the SOH. HF3 and HF4 are very close to the second-use battery SOH, as shown in Fig. 5(c) and (d), respectively. However, HF6, HF7, and HF8 do not track the second-use battery SOH. HF1, HF2, and HF5 are only partially tracking the SOH trend. Obviously, the correlation between HF4 and SOH is the highest, as shown in Fig. 5(d). To be clearer, we introduce the Pearson correlation coefficient to judge the correlation between different HFs and the SOH.

The correlation between SOH and HFs can be evaluated by the Pearson correlation coefficient, which is calculated by

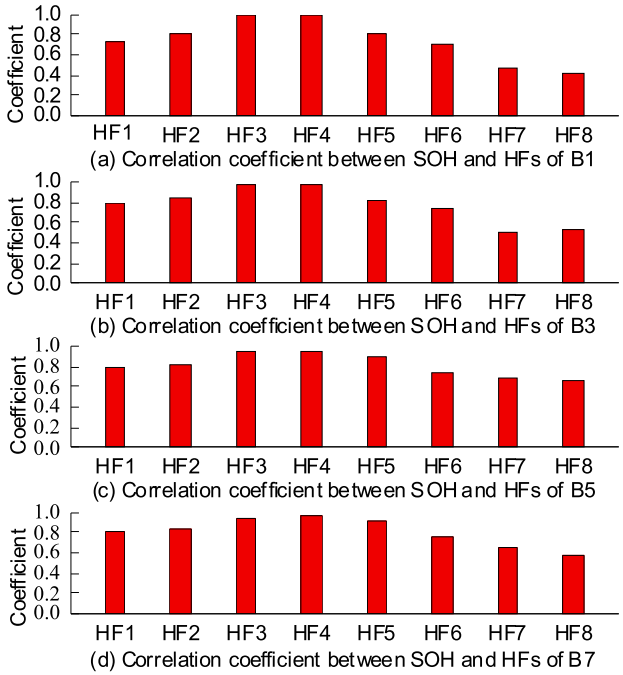

FIGURE 6. The correlation coefficient between SOH and HFs. (a) B1. (b) B3. (c) B5. (d) B7.

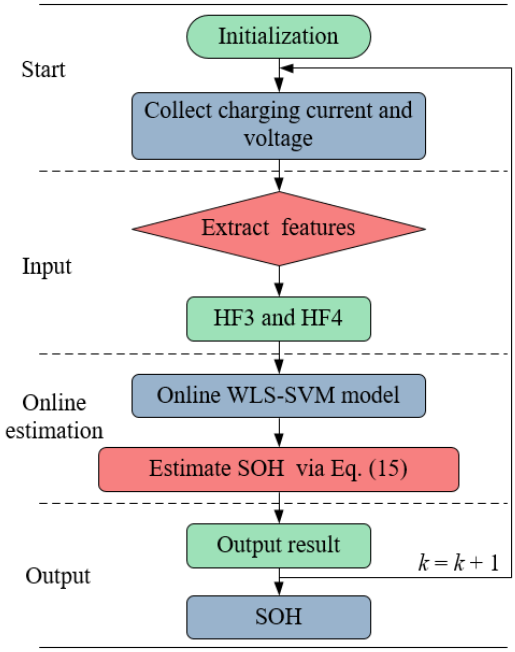

FIGURE 7. Online SOH estimation flowchart based on the WLS-SVM.

the variance and covariance of the two variables. The closer the correlation coefficient is to 1, the better the correlation between the two variables is. The Pearson correlation coefficient can be obtained by:

$$\rho_{SOH,HF} = \frac{Cov(SOH, HF)}{\sqrt{Var[SOH] \cdot Var[HF]}} \tag{2}$$

where $Cov(SOH, HF)$ is the covariance between SOH and HF; $Var[SOH]$ is the variance of SOH; $Var[HF]$ is the variance of HF.

The correlation coefficients calculated using all the training data sets are shown in Fig. 6. The correlation coefficient of HF4 calculated using the data set of battery B1 is 0.988, which is the closest to 1, as shown in Fig. 6(a). The correlation coefficients of HF4 calculated by applying the data sets of battery B3, battery B5, and battery B7 are shown in Fig. 6(b), (c), and (d), respectively. The results of the correlation coefficient show that the correlation coefficients of HF3 and HF4 are high, which are closer to 1 than others. It means that HF3 and HF4 strongly relate to the SOH in second life cycle of batteries. Therefore, HF3 and HF4 are selected as inputs for the proposed method in this paper.

C. WLS-SVM BASED SOH ESTIMATION METHOD

SVMs were first used to solve classification problems [32]. With continuous improvement, SVMs can be applied to solve regression problems. Practical application has shown that SVMs exhibit good performance in regression problems, especially with dealing with high-dimensional function approximation problems [6].

To solve linear regression problems, the best objective function $f(x) = w^T x + b$ can be obtained by an SVM solving the convex quadratic programming problem:

$$\min_{w,b,\xi,\xi^*} \frac{1}{2}\|w\|^2 + C\sum_{i=1}^{n}\left(\xi_i + \xi_i^*\right)$$
$$\text{s.t.} \begin{cases} ((w \cdot x_i) + b) - y_i \le \varepsilon + \xi_i, & i = 1, \cdots, n \\ y_i - ((w \cdot x_i) + b) \le \varepsilon + \xi_i^*, & i = 1, \cdots, n \\ \xi_i \ge 0, \xi_i^* \ge 0, & i = 1, \cdots, n \end{cases} \tag{3}$$

where n is the size of the training data set and $C(C > 0)$ is the penalty parameter. ξ_i and ξ_i^* represent slack variables.

To simplify the problem, the primal function, kernel trick and corresponding constraints can be fed into Eq. (3). Then, the dual problem can be deduced from Eq. (3) by the Karush-Kuhn-Tucker condition and Lagrange multiplier.

$$\min_{a_i^{(*)}} \frac{1}{2}\sum\nolimits_{i,j=1}^{n}\left(a_i^* - a_i\right)\left(a_j^* - a_j\right)(x_i \cdot x_j) + \varepsilon\sum_{i=1}^{n}(a_i^* + a_i) - \sum_{i=1}^{n} y_i(a_i^* - a_i)$$
$$s.t. \begin{cases} \sum_{i=1}^{n}(a_i^* - a_i) = 0 \\ 0 \le a_i^{(*)} \le C \quad i = 1, \cdots, n \end{cases} \tag{4}$$

where a_i and a_i^* are Lagrange multipliers, and only the points that meet the condition $(a_i - a_i^*) \neq 0$ are support vectors. The objective function can be converted as:

$$f(x) = \sum_{i=1}^{n}(a_i^* - a_i)\left(x_i^* \cdot x\right) + b \tag{5}$$

To solve the nonlinear problems and change the complexity of the calculation, the kernel function is introduced into

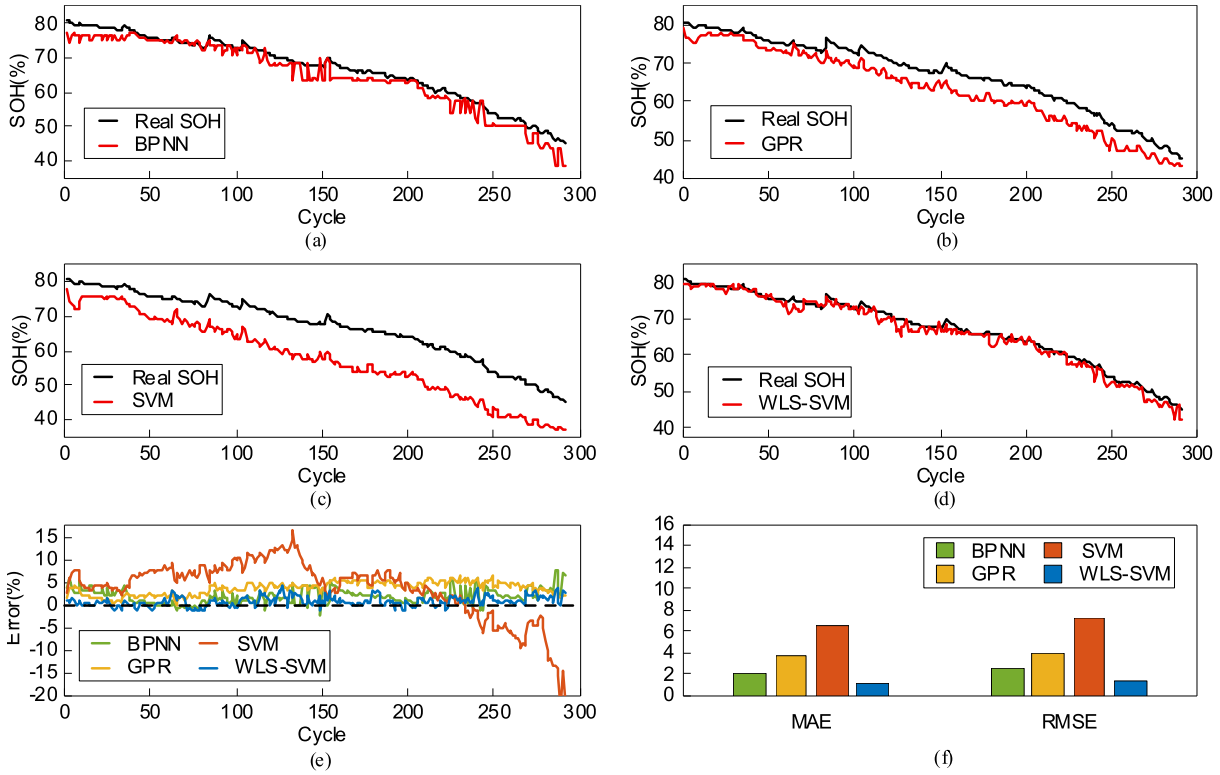

FIGURE 8. SOH estimation results for battery B2. (a) Results for BPNN. (b) Results for GPR. (c) Results for SVM. (d) Results for WLS-SVM. (e) Errors. (f) Statistical indicators.

Eq. (5). The new objective function can be described as:

$$f(x) = \sum_{i=1}^{n} (a_i^* - a_i) k(x_i, x) + b \tag{6}$$

where $K(x_i, x)$ is the kernel function. Due to its good ability to deal with nonlinear problems, the radial basis kernel is one of the most widely used functions [33]; it can be written as:

$$K(x_i, x) = exp\left(-\gamma \|x_i - x\|^2\right) \tag{7}$$

where γ is the radius of the radial basis kernel function. γ is crucial for prediction accuracy. In this paper, the grid search algorithm is used to search the parameter γ, and cross-validation is applied to measure the grid search algorithm on the training set [7]. More concretely, the minimal square error (MSE) is employed to evaluate the selection of γ based on the cross-validation calculation. A suitable γ can be determined when the MSE achieves a minimum.

$$MSE = \frac{1}{l} \sum_{i=1}^{l} (f(x_i) - y_i)^2 \tag{8}$$

where $f(x_i)$ is the estimated SOH, y_i is the actual value, and l is the number of samples.

As seen in Eq. (4), only the training data that satisfy the condition $(a_i^* - a_i) \neq 0$ are used as support vectors. Obviously, not all the training data meet this condition, which brings about the sparseness of the SVM. Generally, the sparseness of an SVM simplifies the calculation as an advantage. However, the sparseness of the SVM results in the dependence of the objective function on the support vectors, which may cause the objective function to fail to characterize the training data set due to the presence of abnormal training points. Therefore, to enhance the robustness of the SVM, the WLS-SVM-based method is employed to train the model and estimate the second-use battery SOH in this paper. Taking all the training data as the support vector, the least squares method improves the SVM by transforming the quadratic programming problem of the SVM into solving linear equations to reduce the computational complexity, and the weight function improves the SVM by weighting the error variables to enhance the robustness. The optimization problem can be transferred to solve the minimum of Eq. (9).

$$J(w, e_i) = \frac{1}{2} \left\| w^2 \right\| + \frac{1}{2} C \sum_{i=1}^{N} v_i e_i^2 \tag{9}$$

The constraint of the equation is as follows:

$$y_i = W^T \varphi(x_i) + b + e_i \tag{10}$$

where v_i is the weight vector of the WLS-SVM. v_i can be obtained as follows:

$$v_i = \begin{cases} 1 & \left| e_i / \hat{S} \right| \leq m_1 \\ \dfrac{m_2 - \left| e_i / \hat{S} \right|}{m_2 - m_1} & m_1 < \left| e_i / \hat{S} \right| \leq m_2 \\ 10^{-4} & otherwise \end{cases} \tag{11}$$

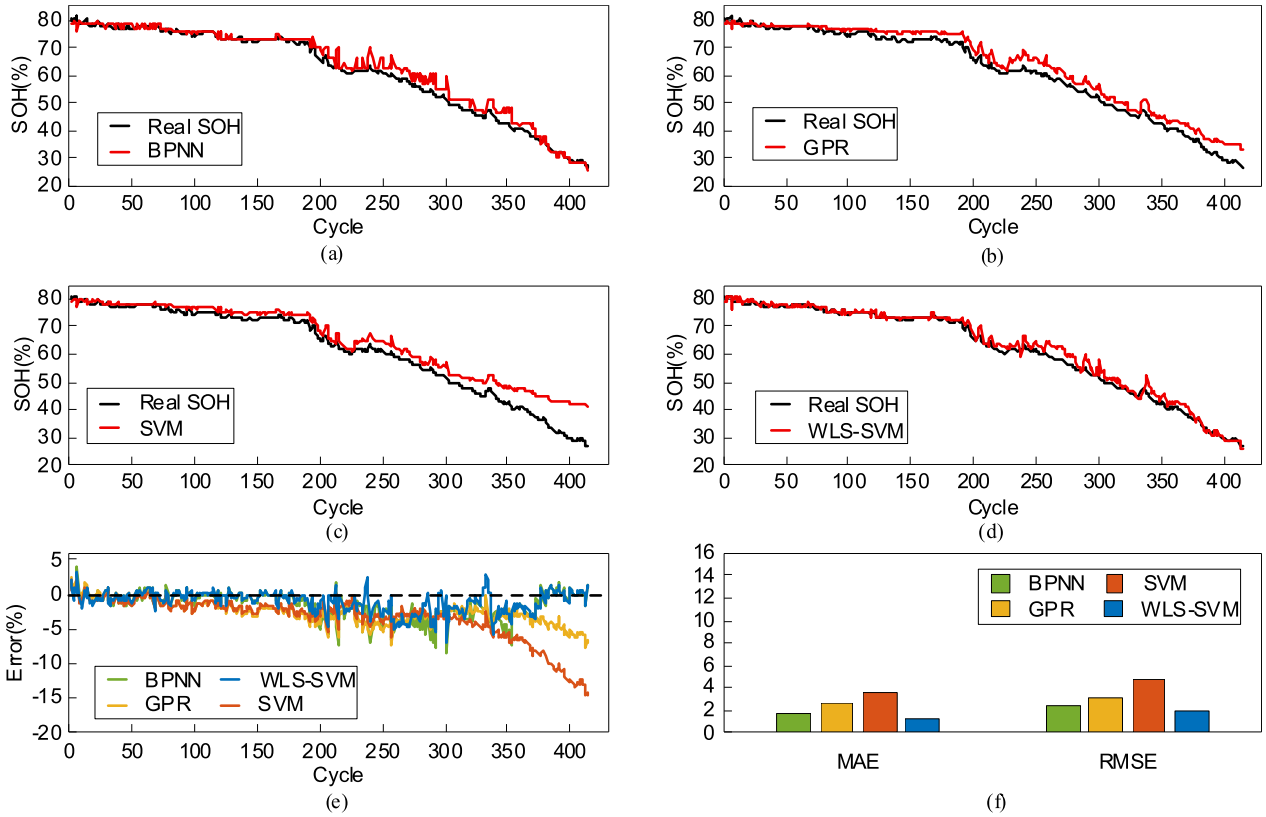

FIGURE 9. SOH estimation results for battery B4. (a) Results for BPNN. (b) Results for GPR. (c) Results for SVM. (d) Results for WLS-SVM. (e) Errors. (f) Statistical indicators.

where $\hat{S} = 1.48MAD(e_i)$ is the standard deviation and $MAD(e_i)$ is the median absolute deviation. To minimize Eq. (9), the Lagrange function can be built by introducing the Lagrange multiplier a_i as follows:

$$\mathcal{L}(w, a_i, b, e_i) = J(w, e_i) + \sum_{i=1}^{N} a_i [y_i - w^T \varphi(x_i) - b - e_i] \quad (12)$$

The Karush-Kuhn-Tucker conditions are given by the following:

$$\begin{cases} \dfrac{\partial L}{\partial \omega} = 0 \Longrightarrow w = \sum_{i=1}^{N} a_i \varphi(x_i) \\ \dfrac{\partial L}{\partial a_i} = 0 \Longrightarrow w^T \varphi(x_i) + b + e_i \\ \dfrac{\partial L}{\partial b} = 0 \Longrightarrow \sum_{i=1}^{N} a_i = 0 \\ \dfrac{\partial L}{\partial e_i} = 0 \Longrightarrow a_i = \gamma v_i e_i \end{cases} \quad (13)$$

Eq. (14) can be obtained by eliminating the variables e_i and w as:

$$\begin{bmatrix} 0 & (l_n)^T \\ l_n & \Omega + I/\gamma v \end{bmatrix} \begin{bmatrix} b \\ a \end{bmatrix} = \begin{bmatrix} 0 \\ y \end{bmatrix} \quad (14)$$

where $a = (a_1, a_2, \ldots a_n)$, $l_n = (1, 1, \ldots 1)^T$, $\Omega_{ij} = \varphi(x_i)^T \varphi(x_j)$, $y = (y_1, y_2, \ldots y_n)$, $v = diag(v_1, v_2 \ldots v_n)$, and I is the identity matrix. The WLS-SVM can be acquired as:

$$\hat{y}(x) = \sum_{i=1}^{N} a_i K(x_i, x) + \mathrm{b} \quad (15)$$

where $K(x_i, x)$ is the kernel function determined by Eq. (7).

Generally, the quadratic loss function is applied in the WLS-SVM, which results in all the training points in the training becoming support vectors. The objective function of the WLS-SVM can weight all the training data sets. Therefore, the WLS-SVM has the competence to efficiently establish a robust model for second-use battery SOH estimation under various working conditions and eliminate the influence of abnormal training data points.

Although the WLS-SVM has more support vectors than an SVM, it is worth noting that the proposed WLS-SVM-based SOH estimation method does not need to retrain the model as the battery working condition changes, which saves considerable time and reduces the computational burden. The procedure for online SOH estimation based on the WLS-SVM is shown in Fig. 7. The inputs for the online WLS-SVM model are HF3 and HF4, namely, the charging capacity from 3.9 V to 3.95 V and from 3.95 V to 4 V under the CC mode. The output of the online WLS-SVM model is the estimated SOH. Next, the results analysis and estimation precision are discussed.

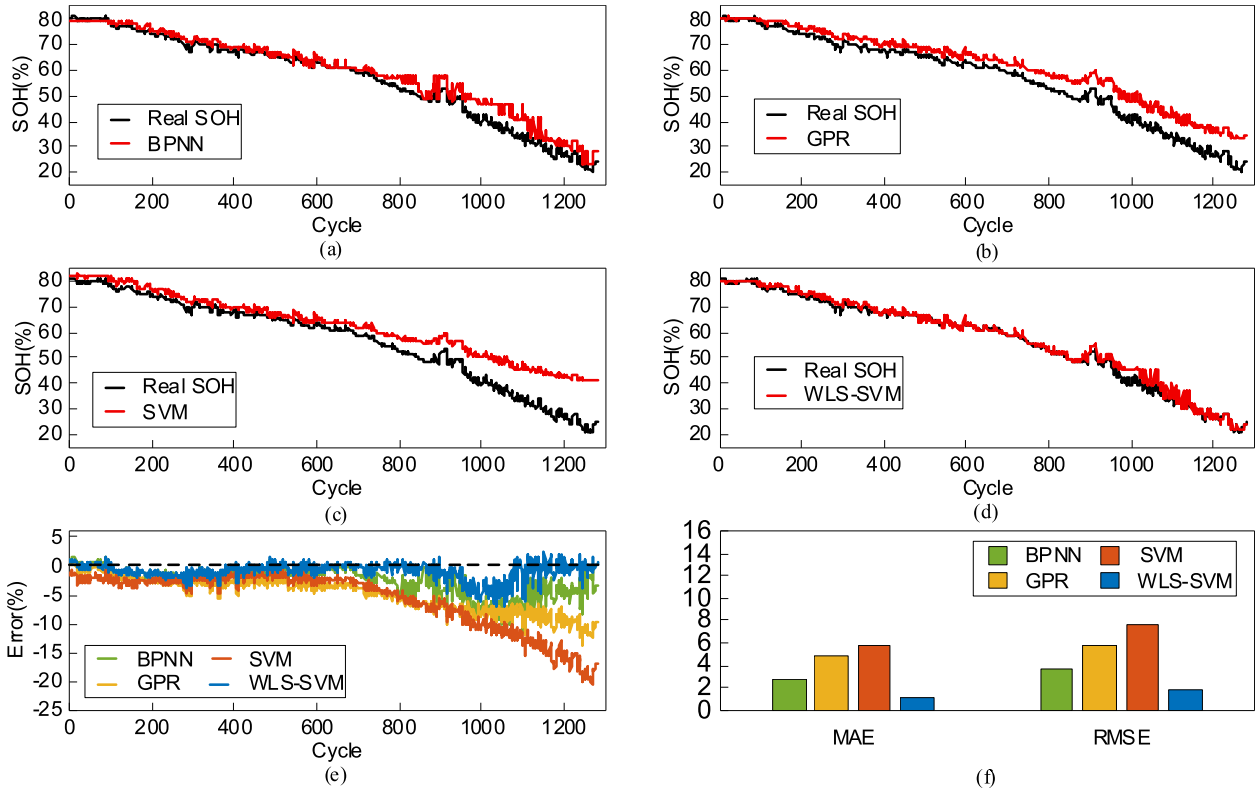

FIGURE 10. SOH estimation results for battery B6. (a) Results for BPNN. (b) Results for GPR. (c) Results for SVM. (d) Results for WLS-SVM. (e) Errors. (f) Statistical indicators.

III. SOH ESTIMATION RESULTS AND DISCUSSION

As mentioned in Section 2.2.1, the data sets for batteries B2, B4, B6, and B8 are applied to test the proposed WLS-SVM-based method. To verify the proposed method, the SOH estimation of second-use batteries is conducted by the proposed method and the most popular methods, including the BPNN-based method, the GPR-based method, and the standard SVM-based method. A BPNN [27] is a multilayer feedforward neural network in an artificial neural network, which is the most representative and extensive approach. The GPR [28], [33]–[35] is designed based on the Bayesian framework [36], [37] and is widely used in prediction tasks [38]–[40]. In SOH estimation, the inputs for the BPNN-based method, the GPR-based method, and the standard SVM-based method are also HF3 and HF4. The output for these data-driven techniques is the estimated SOH. It is necessary to mention that the WLS-SVM, BPNN, GPR, and standard SVM are realized based on the LSSVM, NN, GPML, and LIBSVM toolboxes under MATLAB, respectively.

The training set design concept and the selected features are also verified through the SOH result evaluation. The accuracy of the SOH estimation results is evaluated in terms of the mean absolute error (MAE) and root mean square error (RMSE). Smaller MAE and RMSE values imply better performance. The MAE and RMSE are calculated as:

$$\mathrm{MAE} = \frac{1}{N}\sum_{k=1}^{N}\left|SOH_{k,real} - SOH_{k,estimate}\right| \tag{16}$$

$$\mathrm{RMSE} = \sqrt{\frac{1}{N}\sum_{k=1}^{N}(SOH_{k,real} - SOH_{k,estimate})^2}. \tag{17}$$

The estimation results and errors for battery B2 are shown in Fig. 8. It can be seen that the SOH estimation results for the proposed WLS-SVM-based method are closer to the real SOH. The error value for the standard SVM-based method is the largest, as shown in Fig. 8(e). The standard SVM only selects a few data points that meet the condition $(a_i^* - a_i) \neq 0$ as support vectors for training, as mentioned in Eq. (5). If there are one or several abnormal training points in these data points, the error based on the SVM method will increase. However, the WLS-SVM-based method takes all training data as support vectors and uses a weight function to weight the error variables, which can obtain a SOH estimation with high accuracy. The BPNN-based method and the GPR-based method show similar characteristics to the WLS-SVM-based method, but the errors are larger, as shown in Fig. 8(a) and (b). The MAE and RMSE are applied to assess the results. As shown in Fig. 8(f), the MAE and RMSE of the proposed WLS-SVM-based method are lower than those of the other

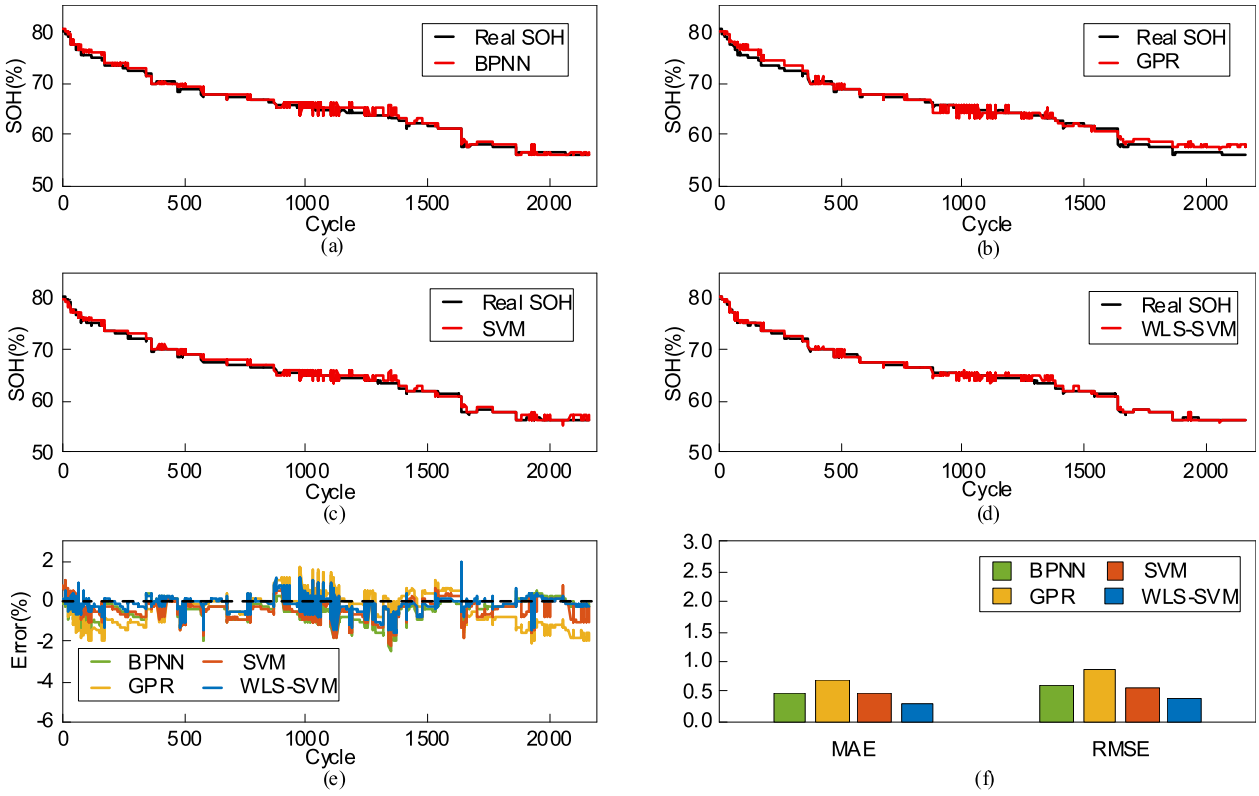

FIGURE 11. SOH estimation results for battery B8. (a) Results for BPNN. (b) Results for GPR. (c) Results for SVM. (d) Results for WLS-SVM. (e) Errors. (f) Statistical indicators.

methods, and the MAE values and RMSE values of the WLS-SVM-based method are under 1.45%.

During the battery test, the discharge current of battery B4 is different from that of battery B2, and the aging rate is also different. The robustness of the proposed method under different conditions can be verified by using the data sets from battery B4 to estimate the SOH. As shown in Fig. 9, the results show superior performance for the proposed WLS-SVM-based method than the other methods in SOH estimation. The SOH estimated by the GPR-based method and standard SVM-based method cannot track the real SOH well after the 225th cycle, as shown in Fig. 9(a) and (c). The SOH error of the BPNN-based method increases when the real SOH fluctuates significantly at the 200th cycle, as shown in Fig. 9(b). Although the real SOH curve is not smooth during all the discharge-charge cycles, as shown in Fig. 9(d), the MAE value and the RMSE value of the WLS-SVM-based method are lower than 1.85%, which implies high accuracy and robustness in SOH estimation.

The material for battery B6 is the same as that for batteries B2 and B4, but its nominal capacity is larger than that of the two batteries. As shown in Fig. 10, the SOH estimation results show that the real SOH can be tracked well by the WLS-SVM-based method, although the nominal capacity is different. However, the SOH errors for the other three methods are relatively large. In addition, as shown in Fig. 10(a), (b), and (c), although the SOH errors are small at the beginning, the SOH estimations by the BPNN-based method, the GPR-based method, and the standard SVM-based method are easily affected by the battery capacity regeneration phenomenon at the 950th cycle. Due to the usage of the weight function, the WLS-SVM method can minimize this impact. As shown in Fig. 10(d) and (e), from the 1000th cycle to the last cycle, the SOH estimation by the WLS-SVM method can come close to the real value. The MAE value and RMSE value can more specifically verify the effectiveness and robustness of the proposed method, and their values are 1.18% and 1.7%, respectively, which are the minimum errors compared with other methods, as shown in Fig. 10(e).

As shown in Fig. 11, although the battery material and charge current of battery B8 are different from those of the other test batteries, by using the data set of battery B8, the WLS-SVM-based method can still obtain a small error, which further validates the high robustness of the proposed method. The MAE value and RMSE value of the proposed WLS-SVM-based method are 0.27% and 0.39%, respectively, as shown in Fig. 11(f). Although the battery test conditions and battery materials have changed, the proposed method can still obtain high estimation accuracy.

In addition, comparing the estimation results of batteries B2, B4, B6, and B8 shows that the accuracy of the proposed method is higher than that of the BPNN-based method and GPR-based method because the WLS-SVM-based method is more suitable for nonlinear problems with little training data.

However, the BPNN-based method and GPR-based method require more training data to obtain good performance.

IV. CONCLUSION

This article proposes an approach for online SOH estimation of second-use lithium-ion batteries based on a weighted least squares support vector machine. In this proposed method, considering that there is little chance for full charge or discharge during practical applications, the charging capacity in a partial voltage range is selected as the key HF by using Pearson correlation coefficient analysis, and the WLS-SVM-based method is used to train the model and estimate SOH online. The proposed method is verified by several second-use lithium-ion battery data sets involving different conditions and different battery materials. The application results show that compared to the BPNN-based method and GPR-based method, the SOH accuracy estimated by the WLS-SVM-based method is the highest because the proposed method is more suitable for nonlinear problems with limited training data. Compared to the standard SVM being easily misled by abnormal training points, the WLS-SVM-based method can improve the SOH estimation performance by weighting the error variables. Additionally, although the test data sets of batteries involve different battery materials and different conditions, the WLS-SVM-based method still performed well. The root mean square error (RMSE) of the SOH estimation with the WLS-SVM-based method for all the test cells is less than 1.85%, whereas the RMSEs of the BPNN-based method, GPR-based method, and standard SVM-based method are within 3.6%, 5.7%, and 7.6%, respectively.

REFERENCES

[1] H. Li, M. Alsolami, S. Z. Yang, Y. Z. M. Alsmadi, and J. Wang, "Lifetime test design for second-use electric vehicle batteries in residential applications," *IEEE Trans. Sustain. Energy*, vol. 8, no. 4, pp. 1736–1746, Oct. 2017.

[2] L. Zhang, Y. Q. Liu, B. B. Pang, B. X. Sun, and A. Kokko, "Second use value of China's new energy vehicle battery: A view based on multi-scenario simulation," *Sustainability*, vol. 314, no. 12, pp. 1–25, 2020.

[3] A. Podias, A. Pfrang, F. D. Persio, A. Kriston, S. Bobba, F. Mathieux, M. Messagie, and L. Boon-Brett, "Sustainability assessment of second use applications of automotive batteries: Ageing of li-ion battery cells in automotive and grid-scale applications," *World Electr. Vehicle J.*, vol. 24, no. 9, pp. 1–15, 2018.

[4] R. Reinhardt, I. Christodoulou, B. A. García, and S. Gasso-Domingo, "Sustainable business model archetypes for the electric vehicle battery second use industry: Towards a conceptual framework," *J. Clean. Prod.*, vol. 254, pp. 1–10, 2020.

[5] R. Reinhardt, I. Christodoulou, S. Gassó-Domingo, and B. A. García, "Towards sustainable business models for electric vehicle battery second use: A critical review," *J. Environ. Manage.*, vol. 245, pp. 432–446, Sep. 2019.

[6] K. Huang, Y. F. Guo, M. L. Tseng, K. J. Wu, and Z. G. Li, "A novel health factor to predict the battery's state-of-health using a support vector machine approach," *Appl. Sci.*, vol. 8, no. 10, pp. 1–21, 2018.

[7] Z. Chen, M. M. Sun, X. Shu, R. X. Xiao, and J. W. Shen, "Online state of health estimation for lithium-ion batteries based on support vector machine," *Appl. Sci.*, vol. 8, no. 6, pp. 1–13, 2018.

[8] J. Kim, H. Chun, M. Kim, J. Yu, K. Kim, T. Kim, and S. Han, "Data-driven state of health estimation of li-ion batteries with RPT-reduced experimental data," *IEEE Access*, vol. 7, pp. 106987–106997, 2019.

[9] J. Kim and B. H. Cho, "State-of-charge estimation and state-of-health prediction of a li-ion degraded battery based on an EKF combined with a per-unit system," *IEEE Trans. Veh. Technol.*, vol. 60, no. 9, pp. 4249–4260, Nov. 2011.

[10] D. Wang, F. Yang, Y. Zhao, and K.-L. Tsui, "Battery remaining useful life prediction at different discharge rates," *Microelectron. Rel.*, vol. 78, pp. 212–219, Nov. 2017.

[11] B. Saha, K. Goebel, S. Poll, and J. Christophersen, "Prognostics methods for battery health monitoring using a Bayesian framework," *IEEE Trans. Instrum. Meas.*, vol. 58, no. 2, pp. 291–296, Feb. 2009.

[12] J. Yu, B. Mo, D. Tang, H. Liu, and J. Wan, "Remaining useful life prediction for lithium-ion batteries using a quantum particle swarm optimization-based particle filter," *Qual. Eng.*, vol. 29, no. 3, pp. 536–546, Jul. 2017.

[13] A. Guha and A. Patra, "State of health estimation of lithium-ion batteries using capacity fade and internal resistance growth models," *IEEE Trans. Transport. Electrific.*, vol. 4, no. 1, pp. 135–146, Mar. 2018.

[14] D. Wang, Y. Zhao, F. Yang, and K.-L. Tsui, "Nonlinear-drifted Brownian motion with multiple hidden states for remaining useful life prediction of rechargeable batteries," *Mech. Syst. Signal Process.*, vol. 93, pp. 531–544, Sep. 2017.

[15] X. Deng, X. Tian, S. Chen, and C. J. Harris, "Deep principal component analysis based on layerwise feature extraction and its application to nonlinear process monitoring," *IEEE Trans. Control Syst. Technol.*, vol. 27, no. 6, pp. 2526–2540, Nov. 2019.

[16] D. Liu, J. Pang, J. Zhou, Y. Peng, and M. Pecht, "Prognostics for state of health estimation of lithium-ion batteries based on combination Gaussian process functional regression," *Microelectron. Rel.*, vol. 53, no. 6, pp. 832–839, Jun. 2013.

[17] Y. Li, S. Zhong, Q. Zhong, and K. Shi, "Lithium-ion battery state of health monitoring based on ensemble learning," *IEEE Access*, vol. 7, pp. 8754–8762, 2019.

[18] P. Guo, Z. Cheng, and L. Yang, "A data-driven remaining capacity estimation approach for lithium-ion batteries based on charging health feature extraction," *J. Power Sources*, vol. 412, pp. 442–450, Feb. 2019.

[19] D. Yang, Y. Wang, R. Pan, R. Chen, and Z. Chen, "A neural network based State-of-Health estimation of lithium-ion battery in electric vehicles," *Energy Procedia*, vol. 105, pp. 2059–2064, May 2017.

[20] Z. He, M. Gao, G. Ma, Y. Liu, and S. Chen, "Online state-of-health estimation of lithium-ion batteries using dynamic Bayesian networks," *J. Power Sources*, vol. 267, pp. 576–583, Dec. 2014.

[21] Z. Ge, "Process data analytics via probabilistic latent variable models: A tutorial review," *Ind. Eng. Chem. Res.*, vol. 57, pp. 12646–12661, Aug. 2018.

[22] E. Schulz, M. Speekenbrik, and A. Krause, "A tutorial on Gaussian process regression: Modelling, exploring, and exploiting functions," *J. Math. Psychol.*, vol. 85, pp. 1–16, Aug. 2018.

[23] X. Feng, C. Weng, X. He, X. Han, L. Lu, D. Ren, and M. Ouyang, "Online state-of-health estimation for li-ion battery using partial charging segment based on support vector machine," *IEEE Trans. Veh. Technol.*, vol. 68, no. 9, pp. 8583–8592, Sep. 2019.

[24] H. Pan, Z. Lü, H. Wang, H. Wei, and L. Chen, "Novel battery state-of-health online estimation method using multiple health indicators and an extreme learning machine," *Energy*, vol. 160, pp. 466–477, Oct. 2018.

[25] X. Li, Z. Wang, L. Zhang, C. Zou, and D. D. Dorrell, "State-of-health estimation for li-ion batteries by combing the incremental capacity analysis method with grey relational analysis," *J. Power Sources*, vols. 410–411, pp. 106–114, Jan. 2019.

[26] R. Xiong, L. Li, and J. Tian, "Towards a smarter battery management system: A critical review on battery state of health monitoring methods," *J. Power Sources*, vol. 405, pp. 18–29, Nov. 2018.

[27] Z. Chen, Q. Xue, R. X. Xiao, Y. G. Liu, and J. W. Shen, "State of health estimation for lithium-ion batteries based on fusion of autoregressive moving average model and Elman neural network," *IEEE Access*, vol. 7, pp. 102663–102678, 2019.

[28] X. Y. Zheng and X. G. Deng, "State-of-health prediction for lithium-ion batteries with multiple Gaussian process regression model," *IEEE Access*, vol. 7, pp. 15383–150394, 2019.

[29] Z. Chu, X. Feng, L. Lu, J. Li, X. Han, and M. Ouyang, "Non-destructive fast charging algorithm of lithium-ion batteries based on the control-oriented electrochemical model," *Appl. Energy*, vol. 204, pp. 1240–1250, Oct. 2017.

[30] J. Meng, L. Cai, D.-I. Stroe, G. Luo, X. Sui, and R. Teodorescu, "Lithium-ion battery state-of-health estimation in electric vehicle using optimized partial charging voltage profiles," *Energy*, vol. 185, pp. 1054–1062, Oct. 2019.
[31] Z. Wang, S. Zeng, J. Guo, and T. Qin, "State of health estimation of lithium-ion batteries based on the constant voltage charging curve," *Energy*, vol. 167, pp. 661–669, Jan. 2019.
[32] C. Cortes and V. Vapnik, "Support-vector networks," *Mach. Learn.*, vol. 20, no. 3, pp. 273–297, 1995.
[33] W. Ye, B. Wang, Y. Liu, B. Gu, and H. Chen, "Deep Gaussian process regression for performance improvement of POS during GPS outages," *IEEE Access*, vol. 8, pp. 117483–117492, 2020.
[34] W. Guo, T. Pan, Z. Li, and S. Chen, "Model calibration method for soft sensors using adaptive Gaussian process regression," *IEEE Access*, vol. 7, pp. 168436–168443, 2019.
[35] W. Kang, J. Xiao, M. Xiao, Y. Hu, H. Zhu, and J. Li, "Research on remaining useful life prognostics based on fuzzy evaluation-Gaussian process regression method," *IEEE Access*, vol. 8, pp. 71965–71973, 2020.
[36] J. Liu and Z. Q. Chen, "Remaining useful life prediction of lithium-ion batteries based on health indicator and Gaussian process regression model," *IEEE Access*, vol. 7, pp. 39474–39484, 2019.
[37] Z. Wang, J. Ma, and L. Zhang, "State-of-health estimation for lithium-ion batteries based on the multi-island genetic algorithm and the Gaussian process regression," *IEEE Access*, vol. 5, pp. 21286–21295, 2017.
[38] P. Cao, Q. Shuai, and J. Tang, "Leveraging Gaussian process regression and many-objective optimization through voting scores for fault identification," *IEEE Access*, vol. 7, pp. 94481–94496, 2019.
[39] B. Jia, J. Zhou, X. Chen, Z. He, and H. Qin, "Deriving operating rules of hydropower reservoirs using Gaussian process regression," *IEEE Access*, vol. 7, pp. 158170–158182, 2019.
[40] L. L. Kang, R. S. Chen, N. X. Xiong, Y. C. Chen, Y. X. Hu, and C. M. Chen, "Selecting hyper-parameters of Gaussian process regression based on non-inertial particle swarm optimization in Internet of Things," *IEEE Access*, vol. 7, pp. 59504–59513, 2019.

WEI XIONG received the M.S. degree in mechanics from Guizhou University, Guizhou, China, in 2011. He is currently pursuing the Ph.D. degree in mechanical engineering with the Wuhan University of Technology, Hubei, China. His current research interests include battery state estimation and battery management systems.

YIMIN MO received the Ph.D. degree in mechanical engineering from the Academy of Mechanical Sciences, Hubei, China, in 1996. He has been a Professor with the Wuhan University of Technology. He is currently the Director of the Wuhan Mechanical Engineering Society. His current research interests include the new energy and battery management systems.

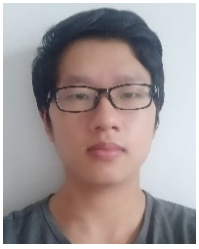

CONG YAN received the B.S. degree in mechanical engineering from the Hubei University of Technology, Wuhan, in 2018. He is currently pursuing the M.S. degree in mechanical engineering with the Wuhan University of Technology, Wuhan. His research interests include battery management systems and battery equalization circuit design.